crystals

MDPI

Article

Accelerated Weathering and Carbonation (Mild to Intensified) of Natural Canadian Silicates (Kimberlite and Wollastonite) for CO_2 Sequestration †

Ye Eun Chai, Salma Chalouati, Hugo Fantucci and Rafael M. Santos *

School of Engineering, University of Guelph, Guelph, ON N1G 2W1, Canada; ychai@uoguelph.ca (Y.E.C.); schaloua@uoguelph.ca (S.C.); hfantucc@uoguelph.ca (H.F.)

* Correspondence: santosr@uoguelph.ca; Tel.: +1-519-824-4120 (ext. 52902)

† Note: Some contents of this paper also appear in the conference proceedings of the 59th Annual Conference of Metallurgists. Reprinted with permission of the Canadian Institute of Mining, Metallurgy and Petroleum.

Abstract: Canada's mineral reserves can play a very important role in curbing climate change if natural alkaline minerals are used for the process of mineral carbonation. In this work, the potential of using two Canadian natural silicates for accelerated carbonation is experimentally assessed: kimberlite mine tailing ($Mg_{0.846}Al_{0.165}Fe_{0.147}Ca_{0.067}SiO_{3.381}$) from the Northwest Territories, and mined wollastonite ore ($Ca_{0.609}Mg_{0.132}Al_{0.091}Fe_{0.024}SiO_{2.914}$) from Ontario. The aim of this work was to evaluate the weathering reactivity and CO_2 uptake capacity via carbonation of these two comminuted rocks, both of which are made up of a mixture of alkaline minerals, under process conditions that spanned from milder to intensified. Research questions addressed include: does kimberlite contain a sufficient amount of reactive minerals to act as an effective carbon sink; is dehydroxylation necessary to activate kimberlite, and to what extent does it do this; do secondary phases of wollastonite hinder its reactivity; and can either of these minerals be carbonated without pH buffering, or only weathered? Incubator, slurry, and pressurized slurry methods of accelerated weathering and carbonation were used, and the effect of the process parameters (temperature, solid-to-liquid ration, reaction time, CO_2 level, pH buffer) on the CO_2 uptake and crystalline carbonates formation is tested. The reacted samples were analyzed by pH test, loss-on-ignition test, calcimeter test, and X-ray diffraction analysis. Results showed that wollastonite ore (rich in fast-weathering $CaSiO_3$) is more suitable for accelerated carbonation than kimberlite tailing (containing slow-weathering hydrated magnesium silicates and aluminosilicates) when only its capability to rapidly form solid carbonates is considered. Incubator and pressurized buffered slurry methods proved to be most effective as under these conditions the precipitation of carbonates was more favorable, while the unbuffered slurry reaction conditions were more akin to accelerated weathering rather than accelerated carbonation.

Keywords: carbon sequestration; CO_2 mineralization; natural silicates; mining residues; solid carbonates

Citation: Chai, Y.E.; Chalouati, S.; Fantucci, H.; Santos, R.M. Accelerated Weathering and Carbonation (Mild to Intensified) of Natural Canadian Silicates (Kimberlite and Wollastonite) for CO_2 Sequestration. *Crystals* **2021**, *11*, 1584. https://doi.org/10.3390/cryst11121584

Academic Editors: Ian Power, Carlos Paulo and Kwon Rausis

Received: 19 September 2021
Accepted: 16 December 2021
Published: 19 December 2021

1. Introduction

As greenhouse gas emissions continue to increase, mineral carbonation has been receiving attention as a solution to mitigate global warming and improve air quality. A recent document released by the Intergovernmental Panel on Climate Change (IPCC) states that limiting global warming to 1.5 °C is possible as opposed to 2 °C, which was agreed to by countries through the Paris Agreement, to prevent climate change to a greater extent [1]. This will require global commitment to achieve zero net emissions by mid-century [1]. Mineral carbonation is a promising solution to this goal as it permanently captures CO_2 while utilizing low-value materials [2,3]. It has also been shown to potentially produce valuable products that can be commercialized to replace traditional carbon-positive materials, such as precipitated carbonates for use as fillers and templates [4,5]. Pan et al. [2] point out

that CO_2 mineralization not only leads to direct CO_2 sequestration but also to substantial amounts of indirect reduction of CO_2 emissions (i.e., avoided emissions), possibly even greater than the sequestered amount in the case of cement replacement.

Mineral carbonation is implemented in one of three ways: ambient or enhanced weathering; engineered accelerated carbonation; and in-situ geological carbonation. While the cost of in-situ mineral carbonation has been suggested by Snaebjörnsdóttir et al. [3] to be starting to become similar to, or lower, than the cost of emissions, the potential of ex-situ mineral carbonation to reduce the net CO_2 emission is questionable, as engineered processes can be energy extensive when they focus on achieving high CO_2 sequestration efficiency. Therefore, economically feasible ex-situ mineral carbonation processes that can be implemented on a large scale need to be developed. Engineered accelerated carbonation uses energy-intensive conditions and/or chemical reagents to enhance the naturally slow reaction kinetics of mineral carbonation [6]. Such methods include simple gas-solid reaction of the silicate mineral and CO_2, and complex multi-step processes [6]. According to past studies, mineral carbonation in an aqueous system shows faster carbonation rates and greater levels of conversion [7,8]. The benefits of engineered accelerated carbonation include flexibility to optimize each step in the process by altering the reaction conditions and the recovery of useful by-products [6]. However, excessive energy consumption during carbonation, which leads to high operating costs, limits engineered accelerated carbonation from being applied on a commercial scale [6]. Moreover, it raises concerns over causing the net release of CO_2, which contradicts the purpose of mineral carbonation to sequester CO_2 [9].

The carbonation of augite and diopside, which are abundant Ca-Mg pyroxenes has been investigated by Monasterio-Guillot et al. [10], by exposing them in hydrothermal conditions to $NaHCO_3$ and Na_2CO_3 as carbonate sources, at a temperature of 150 °C and reaction times of 7, 14, and 28 days. As a result, augite showed higher conversion (~38 wt%) compared to diopside (~15 wt%), and low-magnesium calcite and amorphous silica were the main products of the reaction [10]. The lower conversion of diopside was caused by limited reaction-induced fracturing that creates routes for solution flow, thus restricting the exposure of the unreacted surface inside the crystals [10]. Multiple natural silicate minerals that contain varying mineral composition of mineral phases such as olivine, serpentine, and diopside have been carbonated by Wang et al. [11] under reaction conditions of 175 °C, 34.5 bar CO_2 partial pressure, and concentration of 1.5 M $NaHCO_3$, to investigate their reaction kinetics. The result showed that the overall reaction kinetics of the minerals were dictated by the chemical reaction of olivine dissolution, meaning that higher olivine content led to higher carbonation efficiency, while the other silicate minerals did not significantly affect the reaction [11].

Carbonation of calcium silicates (C_3S, γ-C_2S, C_3S_2, and wollastonite) under reaction condition of 15 vol% CO_2, 29 wt% moisture, and 57 ± 3 °C has also been studied by Ashraf and Olek [12]. All three crystalline calcium carbonate polymorphs (calcite, aragonite, and vaterite) as well as amorphous calcium carbonate (ACC), formed as a result of carbonation, and it was suggested that the ACC formed a composite phase of ACC-SiO_2, which reduced the available surface area for reaction and limited CO_2 diffusion rate into the carbonated matrixes [12]. Carbonation of wollastonite was most effective, though it was also the finest material tested (D_{90} ~10 μm, compared to ~20–50 μm for the other materials). The potential of wollastonite carbonation for CO_2 sequestration has been further demonstrated in other studies [13,14], which have utilized acids (sulfuric acid or hydrochloric acid) for Ca^{2+} leaching and ammonia for neutralization.

Even though wollastonite is seen as one of the most reactive silicate minerals for carbonation, the process is complex as it usually involves three phases (solid, liquid, gas). To better understand the controlling mechanism, a mathematical model of mineral carbonation has developed by Yadav and Mehra [15] that allowed to predict the reaction behavior of the wollastonite in aqueous media. Based on their model, the mineral dissolution was the rate-limiting step of the overall reaction. Efforts have been made to chemically

attempt to overcome this limiting step, such as the use of carbonic anhydrase (CA) and biomimetic metal-organic frameworks (MOF) [16]. However, as is often the case, Di Lorenzo et al. [16] found mixed results (CA was detrimental, and MOF had limited benefit). Difficulties or the impossibility to recover additives from the reacted slurry make this chemical approach questionable. Another approach tested is to conduct wollastonite carbonation in water-bearing supercritical CO_2 [17]. For the carbonation of wollastonite under reaction conditions of 60 °C and 100 bar in water-bearing $scCO_2$, Min et al. [17] have shown that the reaction is limited by the product layer that consisted mostly of amorphous silica, acting as a diffusion barrier to water-bearing $scCO_2$, which is similar to the rate limitation under aqueous conditions.

Carbonation of ultramafic mine tailings has been investigated as well. The mine tailings on site undergo a very slow ambient carbonation reaction; as such, the CO_2 sequestration rates can be enhanced in laboratory settings. The mine tailings sourced from a chrysotile mine in New South Wales, Australia, composed mostly of brucite ($Mg[OH]_2$), showed rapid carbonation under reaction conditions of 10% CO_2 gas and approximately 22 °C; within four weeks, the amount of CO_2 stored in the minerals doubled compared to that stored by passive mineral carbonation on-site for three decades [18]. Similarly, iron ore mining waste composed of mineral phases that are reactive to carbonation, such as wollastonite and diopside, have been carbonated by Ramli et al. [19], and the results showed that smaller particle size, higher temperature, and increased pH enhanced the carbonation efficiency.

Canada's extensive alkaline mineral reserves have the potential to efficiently sequester a large fraction of emissions from the mining, metallurgical, cement, and energy sectors. In this work, the potential of using two Canadian natural silicates for accelerated weathering and carbonation is experimentally assessed: kimberlite mine tailing from the Northwest Territories, and mined wollastonite ore from Ontario. The aim of this work was to evaluate the reactivity and CO_2 uptake capacity of these two comminuted rocks, both of which are made up of a mixture of alkaline minerals, under reaction conditions that spanned from milder to intensified. Research questions addressed include: does kimberlite contain a sufficient amount of reactive minerals to act as an effective carbon sink; is dehydroxylation necessary to activate kimberlite, and to what extent does it do this; do secondary phases of wollastonite hinder its reactivity; and can either of these minerals be carbonated without pH buffering, or only weathered? Two milder methodologies (static incubator and stirred slurry) and an intensified process (pressurized slurry) are tested. The effect of process parameters (temperature, solid-to-liquid ratio, reaction time, CO_2 purity, and pressure) on the CO_2 uptake and crystalline carbonates formations is tested and compared. Pre- and post-carbonation materials are analyzed by pH test, loss-on-ignition test, calcimeter test, and X-ray diffraction (XRD). Figure 1 shows a schematic representation of the mineral carbonation processes and subsequent analyses tested in the present study.

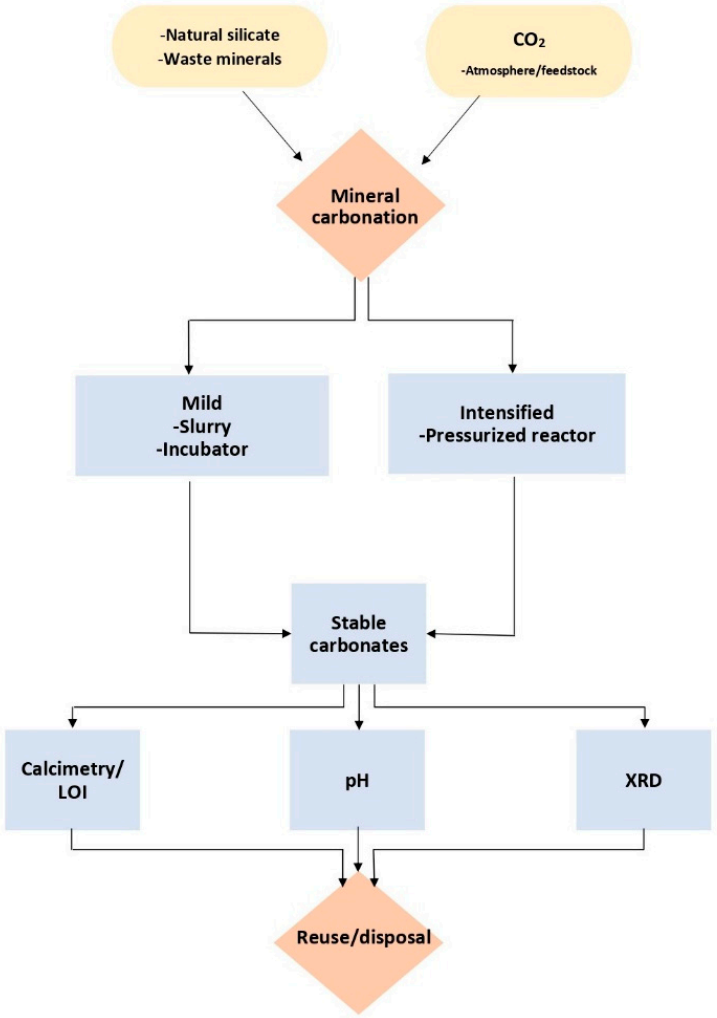

Figure 1. Schematic representation of mineral carbonation processes and materials characterization techniques used in this work.

2. Materials and Methods

2.1. Minerals

2.1.1. Kimberlite Tailings

Kimberlite tailings were sourced from Gahcho Kué Diamond Mine, Northwest Territories, Canada, owned by De Beers Group. Originally, wet kimberlite (classified as finely processed kimberlite, with grain size 3.9–62.5 μm) was received, and it was dried in an oven at 50 °C for 24 h. Once kimberlite was dried, it was disaggregated by a pestle to attain a powdery form. The elemental composition of the kimberlite is 48.4% SiO_2, 27.5% MgO, 9.42% Fe_2O_3, 6.77% Al_2O_3, 3.05% CaO, 1.79% K_2O, 0.919% P_2O_2, and 0.584% Na_2O, determined by X-ray fluorescence (XRF). According to the XRD analysis, unreacted kimberlite is composed mainly of quartz (SiO_2), serpentine ($Mg_3Si_2H_4O_9$), and talc ($Mg_3Si_4O_{10}(OH)_2$). Figure 2 reveals the weathering and carbonation reactions of these two silicate minerals. Its CO_2 content, determined by furnace loss-on-ignition (LOI) was 7.31 wt%, and that after heat treatment (610 °C, 2 h) was 4.74 wt%. Some of the kimberlite samples were heat treated in a furnace at 610 °C for 2 h to dehydroxylate it to potentially improve its reactivity to carbonation [20]. The heat-treated kimberlite samples were tested in only slurry and pressurized carbonation experiments to investigate the effect of heat treatment. According to calcimeter reading, the $CaCO_3$-equivalent carbonate content of the standard kimberlite and heat-treated kimberlite are 19.5 and 9.0 g/kg, respectively. The pH of standard kimberlite and heat-treated kimberlite are 9.2 and 9.0, respectively.

2.1.2. Wollastonite Ore

Wollastonite ore was sourced from Canadian Wollastonite's Ontario mine. The elemental composition of the wollastonite is 52.5% SiO_2, 29.8% CaO, 4.63% MgO, 4.04% Al_2O_3, 3.17% Fe_2O_3, 1.61 wt% K_2O, 1.57% Na_2O, 1.30 wt% SO_3, 0.74% P_2O_5 and trace metals [21]. According to the XRD analysis, unreacted wollastonite is composed mainly of wollastonite ($CaSiO_3$), diopside ($CaMgSi_2O_6$), and quartz (SiO_2) mineral phases. Figure 2 reveals the weathering and carbonation reactions of the two silicate minerals. According to calcimeter reading, the $CaCO_3$-equivalent carbonate content of the wollastonite used was 41.7 g/kg, and its unreacted pH is 10.0.

Silicate mineral	Weathering reaction	Weathering products	Carbonation reaction	Carbonation products
$Mg_3Si_2H_4O_{9(s)}$	$+ H_2O$	$3Mg^{2+} + 6OH^- + 2SiO_{2(s)}$	$+ 3CO_3^{2-} + 6H^+ + 9H_2O$	$3MgCO_3{\cdot}5H_2O_{(s)} + 2SiO_{2(s)}$
$Mg_3Si_4O_{10}(OH)_{2(s)}$	$+ 2H_2O$	$3Mg^{2+} + 6OH^- + 4SiO_{2(s)}$	$+ 3CO_3^{2-} + 6H^+ + 9H_2O$	$3MgCO_3{\cdot}5H_2O_{(s)} + 4SiO_{2(s)}$
$CaSiO_{3(s)}$	$+ H_2O$	$Ca^{2+} + 2OH^- + SiO_{2(s)}$	$+ CO_3^{2-} + 2H^+$	$CaCO_{3(s)} + SiO_{2(s)} + 2H_2O$
$CaMgSi_2O_{6(s)}$	$+ 2H_2O$	$Ca^{2+} + Mg^{2+} 4OH^- + 2SiO_{2(s)}$	$+ 2CO_3^{2-} + 4H^+ + H_2O$	$CaCO_{3(s)} + MgCO_3{\cdot}5H_2O_{(s)} + 2SiO_{2(s)}$

Figure 2. Schematic representation of mineral weathering and mineral carbonation reactions of the two main silicate minerals in the kimberlite and wollastonite ores used in this work; lansfordite is assumed to be the magnesium carbonate forming, but other carbonates (e.g., nesquehonite, hydromagnesite or dolomite) are also possible (which would alter the reactants shown).

2.2. Accelerated Weathering and Carbonation Experiments

2.2.1. Incubator Process

To conduct accelerated weathering and carbonation under static conditions, a CO_2 incubator (Binder (Tuttlinger, Germany) C170) was used. Experimental procedures and conditions were adapted from past studies [22,23]. Reaction temperatures of 35 and 50 °C, CO_2 levels of 10, 15, and 20% (0.10, 0.15, 0.20 atm CO_2), and moisture contents of 10, 15, 20, and 30 wt% were tested. In four stainless steel trays, 60 g of kimberlite or wollastonite was wetted using ultrapure water (18.2 MΩ·cm) to attain moisture contents of 10, 15, 20, and 30 wt% for each sample and spread onto the trays. The trays were put in the CO_2 incubator for 6 consecutive nights (144 h), while 10 g of intermediate samples were collected every 24 h. When collecting the intermediate samples, the content in each tray was lightly deagglomerated by using a pestle and re-wetted to maintain its initial moisture content. The collected samples were put in a crucible and placed in an oven at 60 °C for 24 h for drying.

2.2.2. Slurry Process

To conduct accelerated weathering and carbonation under dynamic conditions, a stirred slurry process was conducted under atmospheric pressure and the reaction conditions used were adopted from a study that tested carbonation of Ca-rich materials such as lime, wollastonite, and steel slags [24]. The reaction temperature of 40, 50, and 60 °C, and reaction times of 1, 2, and 4 h were tested. A 2 L beaker was filled with 1 L of ultrapure water (18.2 MΩ·cm) or sodium hydroxide (NaOH) solution (0.64 M) and placed on a hot

plate (IKA (Staufen German) IKA Plate). In the beaker, a CO_2 injecting tube, connected to a CO_2 gas cylinder (99.0 vol%), was put in and the gas was supplied at a rate of ~2 L/min, monitored by a rotameter. At the same time, a thermocouple measured the temperature inside the beaker and a mechanical stirrer (IKA (Staufen, Germanu) RW 20) operated at a stirring speed of 395–400 rpm. To ensure that the water was saturated with CO_2, pH was measured using a pH meter until it stabilized. Once the pH stabilized and the predetermined reaction temperature was reached, 50 g of solids was added to the beaker to initiate the reaction. After the reaction time, the carbonated slurry was filtered using a filter paper (Whatman (Maidstone, UK) 2V 150 mm (1202-150)) and the recovered solids were dried in an oven at 60 °C for 24 h. The filtrate may be reused as a liquid for multiple experiments, however, in this research, it was disposed of after single use. The samples that used NaOH were washed with ultrapure (18.2 MΩ·cm) water prior to drying.

2.2.3. Pressurized Slurry Process

For pressurized slurry weathering and carbonation, a stirred batch reactor that is capable of handling high temperature and high pressure was used. A 1 L bolted closure pressure vessel (Parker Autoclave Engineers (Erie, PA, USA)) made of Inconel was filled with 100 g of solids and 800 mL of liquid, ultrapure water (18 MΩ·cm) or 0.64 M NaOH. The reactor was pressurized with CO_2 from a gas cylinder (99.0 vol%) and heated using a heating jacket until the pressure inside the vessel reached 60 bar and the temperature reached 200 °C. These NaOH concentration and temperature were chosen as they contributed to achieving the highest carbonation extent of olivine by Santos et al. [25], while it was demonstrated that the carbonation extent of olivine increased linearly with increasing CO_2 partial pressure, reaction time, and solid to liquid ratio. Once such initial reaction conditions were achieved, the reaction proceeded for 4 h. The mixture in the vessel was being stirred at 1000 rpm using a straight-blade-turbine impeller, also made of Inconel, throughout the reaction. After the reaction time, the vessel was cooled and depressurized and the slurry from the vessel was filtered using a filter paper (Whatman (Maidstone, UK) 2 V 150 mm (1202-150)) and recovered solids were dried in an oven at 105 °C for 24 h.

2.3. Analytical Tests

2.3.1. pH Test

A pH test was done using a pH meter (Fisher Scientific (Waltham, MA, USA) Accumet AE150) on all samples collected including intermediate samples from incubator carbonation experiments. Before the test, the pH meter was calibrated using pH 7.00 and 10.01 buffers. Two g of dried sample was ground and put into a 250 mL beaker and 200 mL of ultrapure water (18.2 MΩ·cm) was added. While the content in the beaker was being mixed by a magnetic stirrer, the pH was measured until it stabilized.

2.3.2. Furnace Test

Loss on ignition (LOI) of carbonated kimberlite and wollastonite samples was determined through furnace test. The furnace test was conducted at two temperatures, 300 and 950 °C; 300 °C was used to remove bonded water that could have formed during carbonation and 950 °C was used to determine the weight loss from CO_2 released from the samples. To get the net CO_2 released sequestered, the mass loss for carbonated samples in this temperature range was deducted by the mass loss in the same temperature range for fresh kimberlite. For testing, 2 g of sample was placed in a small crucible and placed in a furnace set to 300 °C. Once the furnace reached 300 °C, a timer started for 10 min. After the 10 min, the sample was taken out, weighed, and put back in the furnace. Once the furnace reached 950 °C, the timer started for another 10 min. After the 10 min, the sample was taken out and weighed. The percentage (wt%) of CO_2 released in each sample was calculated using Equation (1), where P represents the percentage of CO_2 released, in wt%;

$m_{300°C}$ and $m_{950°C}$ represent masses measured after 10 min of being placed in the furnace at 300 and 950 °C; and $m_{initial}$ represents mass measured prior to being place in the furnace.

$$P(wt\%) = \frac{m_{300°C} - m_{950°C}}{m_{initial}} \times 100\% \quad (1)$$

2.3.3. Calcimeter Test

Calcimetry was used to determine the inorganic carbon content (as $CaCO_3$-equivalent carbonate content) in unreacted minerals, in incubator carbonated wollastonite collected after 144 h, in all slurry carbonated wollastonite samples, and in pressurized slurry carbonated kimberlite samples, using a calcimeter (Eijkelkamp (Giesbeek, The Netherlands) 08.53). The calcimeter consists of 5 sealed Erlenmeyer flasks, each of them connected to a graduated water-filled manometer-style column that measured the volume of the released CO_2 [26]. Prior to sample testing, pure $CaCO_3$, a solid standard, was tested twice following the same procedure, and blank determinations were also conducted. To prepare samples for testing, 5 g of carbonated sample was suspended in 20 mL of ultrapure water (18.2 MΩ·cm) in the Erlenmeyer flask, and 7 mL of 4 M HCl contained in a small open test tube was carefully placed standing within the same flask [26]. After sealing the Erlenmeyer flask, it was swirled to knock down the HCl test tube and the reaction was initiated and released CO_2. With the measured released CO_2 volume, the amount of $CaCO_3$-equivalent carbonate in the samples was calculated using Equation (2), sourced from the equipment manual, where W_{CaCO3} represents carbonate content in $g_{carbonate}/kg_{sample}$ and m_1 and m_2 represent the mass of sample used and mean mass of pure $CaCO_3$ used, respectively, in grams; V_1 and V_2 represent the volume of CO_2 released by the sample and mean volume of CO_2 released by the standards, respectively, in milliliters; V_3 represents mean volume change in the blank determinations, in milliliters; and W_{H2O} represents the water content of the dried sample determined according to ISO 11465, in wt%. As the carbonated samples were dried before storing, W_{H2O} value was assumed to be 0 for all calculations.

$$W_{CaCO_3} = 1000 \times \frac{m_2(V_1 - V_3)}{m_1(V_2 - V_3)} \times \frac{100 + W_{H_2O}}{100} \quad (2)$$

2.3.4. XRD Analysis

For incubator carbonation samples collected after 144 h and all slurry carbonation samples, XRD analysis was conducted for phase identification of the crystalline carbonates formed. Before analysis, the samples were ground using a pestle to remove any clustered particles and pressed in a cavity. The sample was loaded into the reflection-transmission spinner of the equipment (Malvern Panalytical (Almelo, The Netherlands) Empyrean XRD Diffractometer), and each sample was irradiated for 20 to 60 min. For data analysis and peak identification, software Data Viewer and HighScore Plus (Malvern Panalytical (Almelo, The Netherlands)) were used. The XRD diffractograms were plotted using Microsoft Excel.

3. Results and Discussion

3.1. pH Test

The results of the pH test were analyzed to compare the effects of process conditions such as temperature, CO_2 level, and moisture content. The pH of unreacted kimberlite, heat-treated kimberlite, and wollastonite were 9.2, 9.0, and 10.0, respectively. The results of kimberlite incubator carbonation did not show a significant change in pH at essentially all process conditions, with pH measurements ranging between 8.9–9.3 (Figure S1 in the Supplementary Material). However, kimberlite samples with higher moisture contents (20 wt%) that carbonated at 35 °C demonstrated the lowest pH (pH 9.16–9.03) throughout the experiment (Day 1–6) (Figure S1), possibly suggestive of improved carbonation when the CO_2 solubility is highest and more aqueous medium is available.

The wollastonite samples carbonated via incubator carbonation showed a general trend where pH decreased according to the reaction time (Day 1–6) for all combinations

of process conditions, with minor changes in pH ranging between 9.7–9.9 (Figure 3, and Figure S2 in the Supplementary Material). Figure 3 illustrates pH measurements taken on Day 1 and Day 6 of the wollastonite samples carbonated in the incubator under 0.10 CO_2, which shows that pH is decreased on Day 6 in Figure 3a,b, compared to those of Day 1.

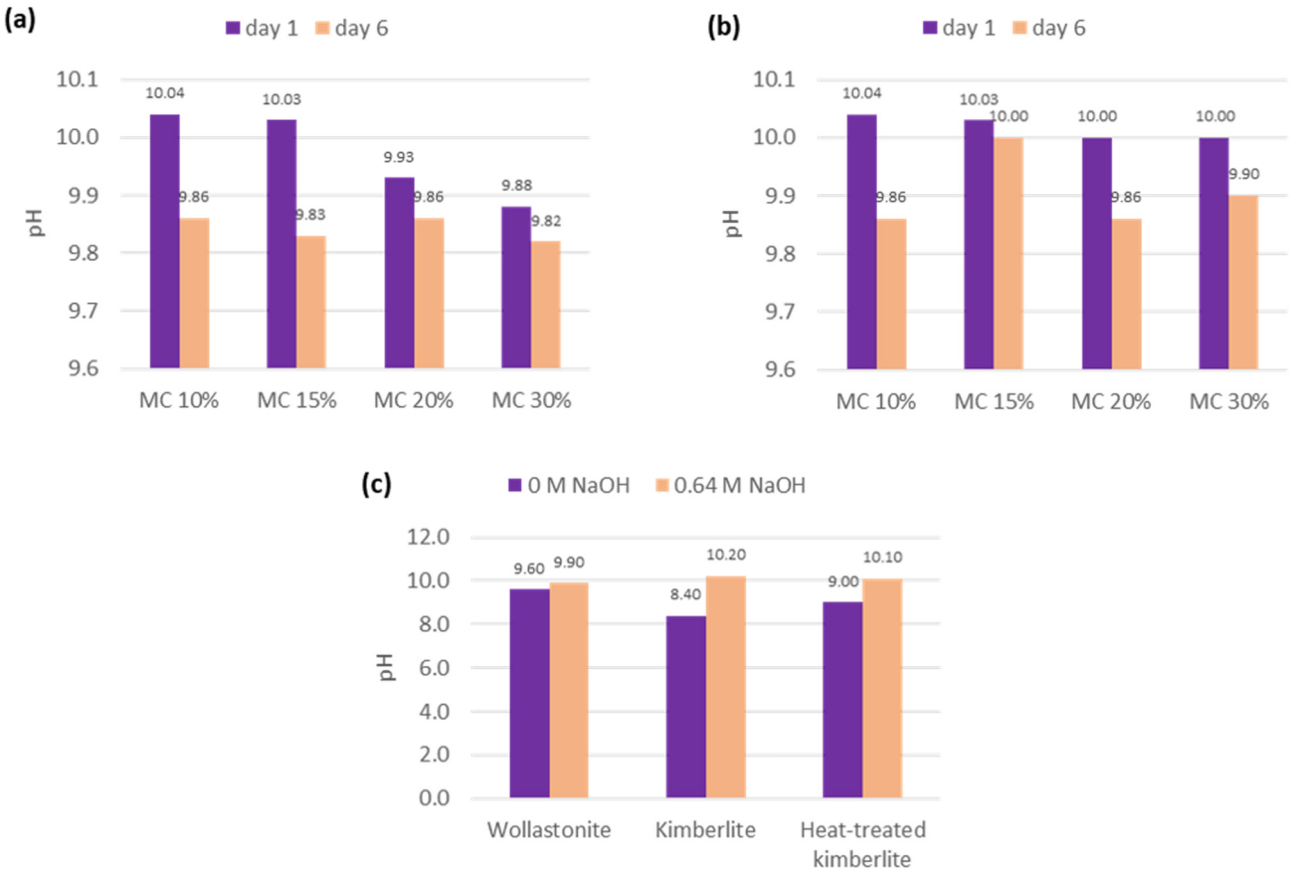

Figure 3. The pH of carbonated wollastonite after incubator carbonation (24 h and 144 h) at 10% CO_2 and reaction temperatures of (**a**) 35 °C and (**b**) 50 °C where MC represents moisture content; (**c**) pH of carbonated wollastonite and kimberlite through pressurized carbonation (4 h, 200 °C, 60 bar CO_2). The pH of unreacted kimberlite, heat treated kimberlite, and wollastonite are 9.2, 9.0, and 10.0, respectively.

The pH measurements of the samples obtained through slurry carbonation using ultrapure water showed lower pH than those obtained through incubator carbonation (Figure S3 in the Supplementary Material). Kimberlite samples carbonated without heat treatment showed lower pH (8.1–8.7, Figure S3a)) compared to the samples that received heat treatment (pH 9.0–9.5, Figure S3b). Such results suggest that heat treatment had an unintended negative effect on weathering and carbonation, which is later assessed by the other analyses. For wollastonite samples, pH decreased with increasing reaction time while variation in temperature did not show a significant trend (Figure S3c). The pH values of slurry carbonated wollastonite were lower than those for incubator carbonation wollastonite, suggesting a greater degree of reaction. Overall, it was noted that both incubator and slurry carbonations were more greatly affected by reaction time than to temperature.

Samples that were slurry carbonated in NaOH solution showed an inconsistent trend (Figure S4 in the Supplementary Material). The pH of the carbonated materials did not noticeably change, with variations in reaction temperature and prolonged reaction time showing a very minor change in pH. This could indicate that the sodium from the solution precipitated during drying in the oven, making the samples more basic than the basicity of the reacted minerals. Similar to the results of mild carbonation, the pH of the carbonated materials from pressurized carbonation did not effectively indicate carbonation for samples

prepared in the presence of NaOH (Figure 3c). Compared to the pH of unreacted materials, pH changes without NaOH were similar to those seen under milder slurry carbonation (Figure 3c).

The pH test results of carbonated kimberlite and wollastonite provide some suggestion of weathering or carbonation having occurred but are less useful for predicting the level of carbonation achieved. In the case of very alkaline materials (>pH 11), such as slags, bottom ashes, and fly ashes, the greater reduction in basicity indicates more clearly and confidently the carbonation effect [22]. However, unreacted kimberlite and wollastonite used in this research had pH of 9.2 and 10.0, respectively, which are similar to the pH of carbonate products. It should be noted that pH reduction is expected to level off once the mineral becomes significantly carbonated, reaching a value close to that of the predominant carbonate phase that forms. Thus, additional tests are needed to confirm if the minerals were weathered or carbonated under the conditions tested.

3.2. Furnace and Calcimeter Tests

The CO_2 and carbonate contents in the carbonated samples determined via furnace and calcimeter tests fill the uncertainties found in the pH test results. When considering the numerical values of CO_2 uptake determined by LOI, it is important to consider the LOI of the unreacted materials, which were 7.31 wt% for kimberlite and 4.74 wt% for heat-treated kimberlite. The results of incubator carbonation of the kimberlite samples showed that at the lower temperature (35 °C, Figure 4a), the samples with higher moisture content sequestered a slightly greater amount of CO_2. In contrast, at the higher temperature (50 °C, Figure 4b), samples with higher moisture content sequestered less amount of CO_2. These trends are in agreement with the pH trends presented earlier, even though the changes in values in small. In fact, it is now confirmed that the net CO_2 sequestered by kimberlite through incubator is minimal (<1.0 wt%). This minimal effect of carbonation can be explained by the stagnant water created within the pores surrounding the mineral particles, hindering CO_2 from contacting the alkaline earth metal ions for reaction, but can also be a function of low reactivity of the hydrated silicates and aluminosilicate minerals that make up the kimberlite tailings under the incubator conditions. Thus, analysis of reactivity under more intense conditions is later discussed.

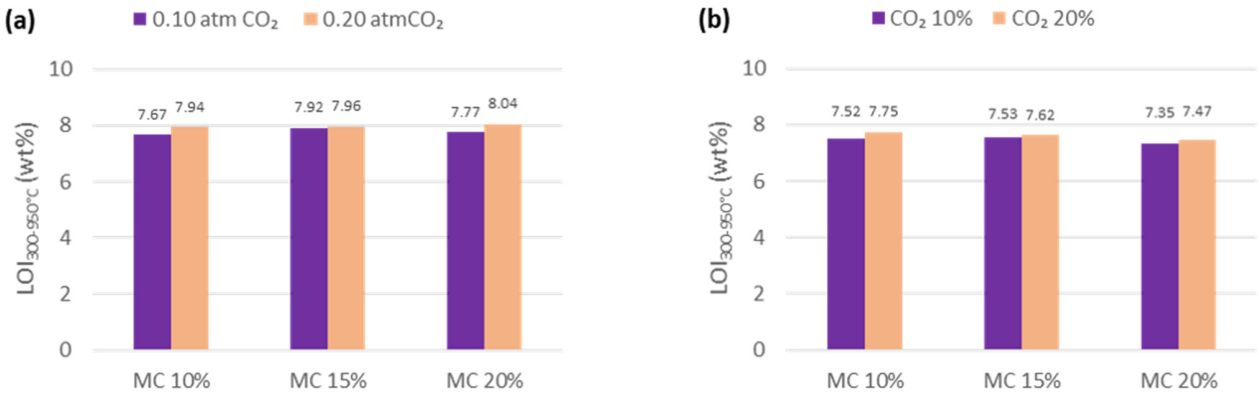

Figure 4. CO_2 content ($LOI_{300–950°C}$) of incubator carbonated (144 h) kimberlite at (**a**) 35 °C and (**b**) 50 °C where MC represents Scheme 2 content ($LOI_{300–950°C}$) of unreacted kimberlite is 7.3 wt%.

The results of slurry carbonation of the kimberlite samples (Figure 5) showed a significant difference depending on the presence of heat treatment. Most kimberlite samples without heat treatment turned out to have a negative net CO_2 sequestered, while the samples with heat treatment had an average of 1.0 wt% net CO_2 sequestered (Figure 5a,b). Variation in process conditions did not infer any significant trends. This suggested that the kimberlite without heat treatment was only weathered (i.e., lost some of its original carbonate content), while the heat-treated kimberlite gained carbonate content. This trend

differs from the incubator results because incubator samples are dried as is (with the aqueous medium), while slurry samples are filtered. After all, the aqueous medium in slurry carbonation is more acidic due to greater CO_2 partial pressure (1.0 atm versus 0.1–0.2 atm), and because the incubator reaction was significantly longer (144 h versus 4 h). It was therefore desired to see the effect of NaOH on slurry carbonation (to buffer pH and increase CO_2 solubility in the aqueous medium).

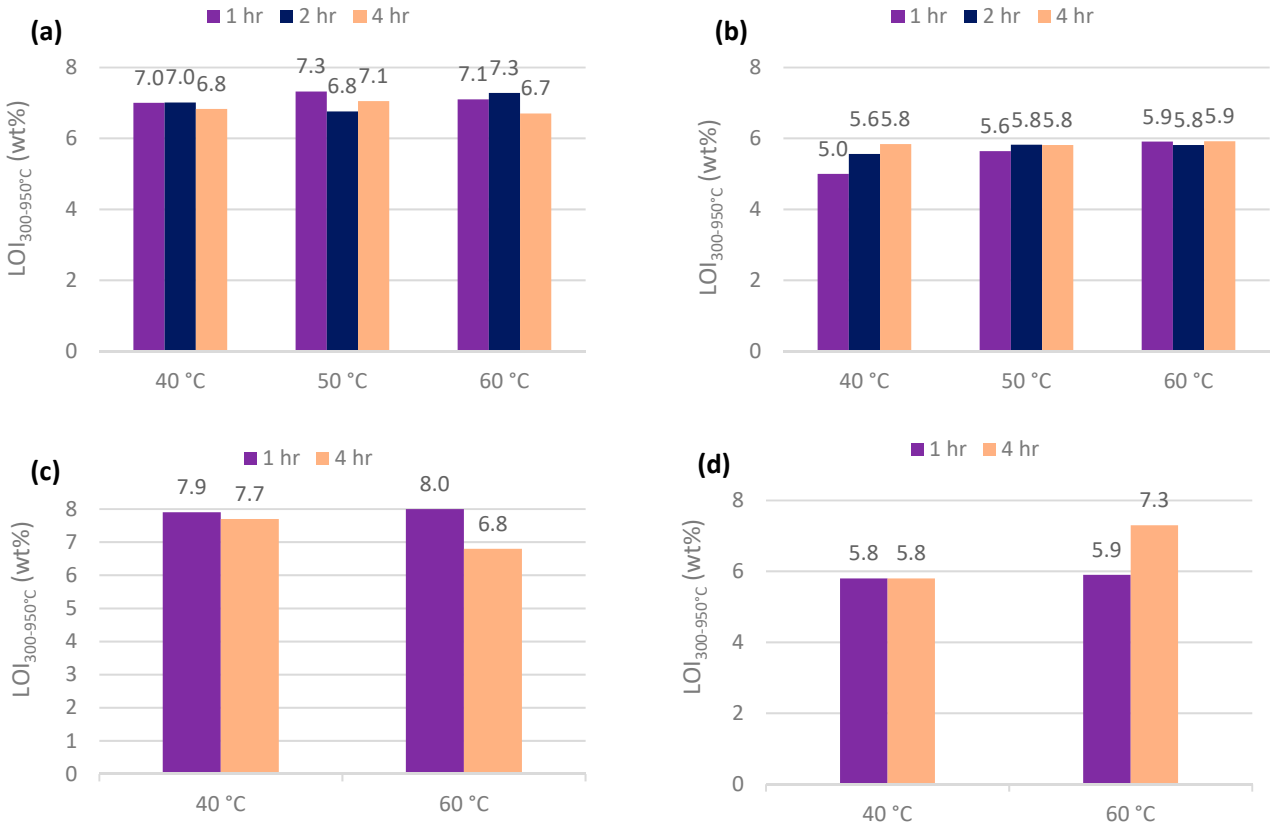

Figure 5. CO_2 content ($LOI_{300–950°C}$) of slurry carbonated (**a**) kimberlite and (**b**) heat treated kimberlite in ultrapure water and (**c**) kimberlite and (**d**) heat treated kimberlite in 0.64 M NaOH. CO_2 content ($LOI_{300–950°C}$) of unreacted kimberlite and heat-treated kimberlite are 7.3 and 4.7 wt%, respectively.

With NaOH addition, sequestered CO_2 content increased significantly, verifying the effectiveness of the slurry carbonation, which was not clearly shown with the pH test results. When Figure 5a,c is compared, it can be seen that the CO_2 content increased for all combinations of reaction conditions, by 0.7 wt% on average. Moreover, the effectiveness of NaOH is shown in the heat-treated kimberlite as well (Figure 5b versus Figure 5d), but only in the sample reacted for 4 h at higher temperature (60 °C). The effect that the NaOH has on carbonation is the buffering of the basicity of the environment. Mineral carbonation occurs at high pH (>9) caused by the high carbonate ions (CO_3^{2-}) concentration [27]. At lower pH, carbonic acid dissociation is limited, with bicarbonate ions being dominant at near-neutral pH, and undissociated carbonic acid dominant at acidic pH. This pH-dependent transition is dictated by the pKa values of carbonic acid, namely 6.351 (H_2CO_3/HCO_3^-) and 13.329 (HCO_3^-/CO_3^{2-}). To elevate the pH of the acidic CO_2 dissolved water, buffering the pH is necessary to initiate carbonation, especially when mild reaction conditions are used. From the results of the furnace test, it was learned that kimberlite can be carbonated using the incubator carbonation method, although the net CO_2 sequestration is small, and that the slurry carbonation method is ineffective to carbonate kimberlite, however, by using 0.64 M NaOH as the carbonation medium, the carbonation extent can at least match that of the incubator process (but in far less time). It was thus of interest to see if pressurized

slurry carbonation, at significantly higher temperatures and pressures, could outperform incubator and slurry carbonation results, and this is presented later.

Figure 6a–d illustrates the carbonate content ($g_{carbonate}/kg_{sample}$) of incubator and slurry carbonated wollastonite. The carbonate content of unreacted wollastonite is 41.7 g/kg. As wollastonite is naturally a more reactive material due to its Ca content compared to kimberlite, the wollastonite samples carbonated through the incubator carbonation method showed a significant increase in the carbonate content and a much more significant change than that seen for the LOI of kimberlite. When Figure 6a,b is compared, a greater number of carbonates formed at higher temperature (50 °C) than lower (35 °C) at all combinations of process conditions. Specifically, when wollastonite with a moisture content of 30 wt% was carbonated with a CO_2 level of 0.20 atm (20%) at 50 °C, an increase of 87% in carbonate content occurred compared to that carbonated at 35 °C. This result is interesting as the solubility of CO_2 decreases with increasing temperature [28]. So improved mineral reactivity, and possibly the transport of ions through diffusion-limiting layers, make up for the lower CO_2 solubility in the case of wollastonite, which is the opposite seen for kimberlite. This suggests that the limiting mechanisms differ for the two minerals and should be the subject of more detailed investigation. However, at the optimal temperature for wollastonite (Figure 6b), the effect of CO_2 level and moisture content was similar to that in the case of kimberlite at its optimal temperature (Figure 4a), with a higher CO_2 level and moisture content contributing to slightly greater CO_2 uptake.

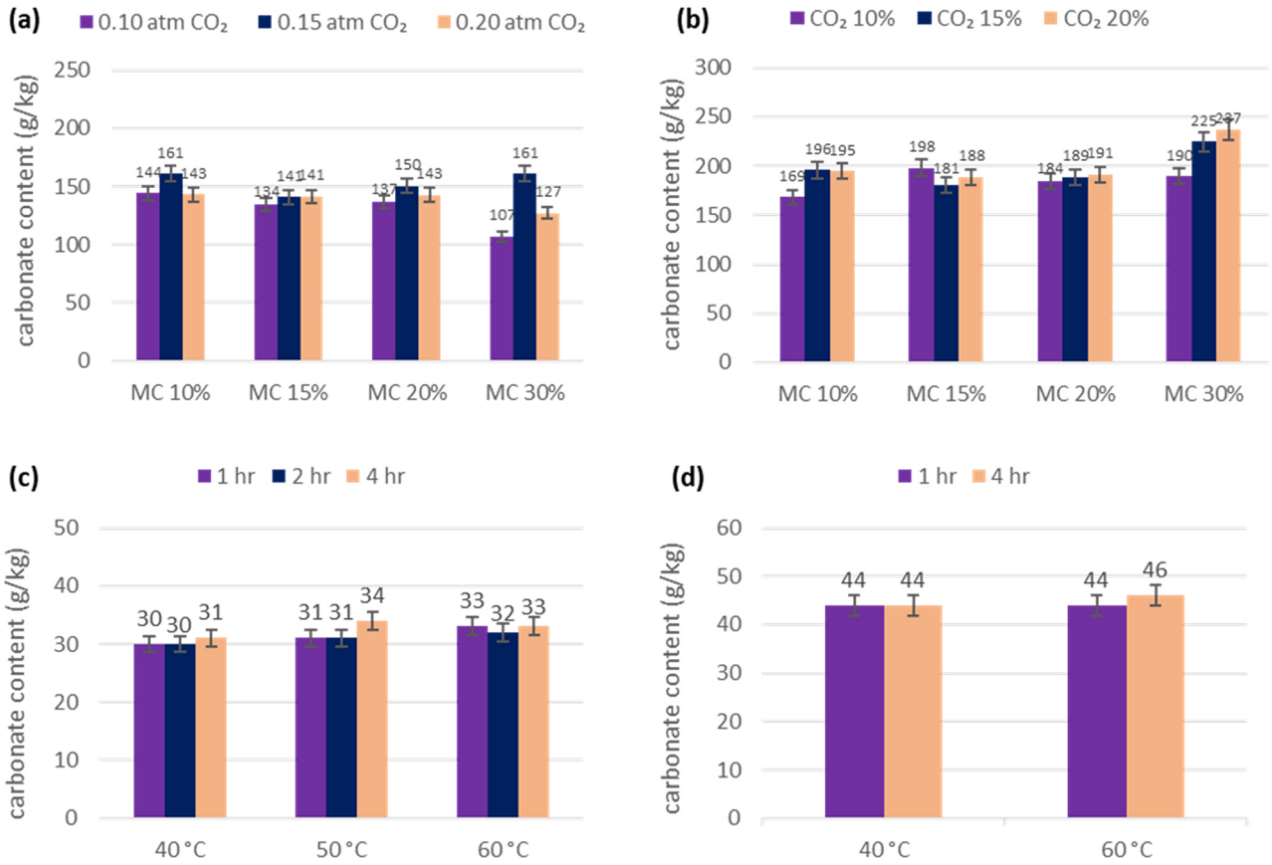

Figure 6. Carbonate content of incubator carbonated (144 h) wollastonite at (**a**) 35 °C and (**b**) 50 °C (calcimeter mean accuracy: ±4.2%) and slurry carbonated wollastonite in (**c**) ultrapure water and (**d**) NaOH (calcimeter mean accuracy: ±4.7%). Carbonate content of unreacted wollastonite is 41.7 g/kg.

According to Figure 6c, slurry carbonated wollastonite had carbonate content ranging between 30–34 g/kg. These values were unexpected as they are actually lower than the carbonate content of unreacted wollastonite (41.7 g/kg), meaning that carbonation did

not occur and some carbonates that existed in unreacted wollastonite decomposed during slurry carbonation. It is interesting to note that the pH of slurry carbonated wollastonite (Figure S3c) was lower than that of incubator carbonated wollastonite (Figure S2) because it is understood that carbonation leads to a reduction in basicity. If carbonation did not happen during slurry carbonation, the pH should have remained high, close to 10.0, which is the pH of unreacted wollastonite. It thus appears that wollastonite did weather during slurry carbonation, but solid carbonates did not form is appreciable amount (more on this in the XRD analysis discussion). Even with the use of 0.64 M NaOH in slurry carbonation, the carbonation performance of wollastonite only increased by 12.8 g/kg on average (Figure 6d), barely surpassing the value of unreacted wollastonite. Here again, it appears that weathering rather than carbonation was the dominant reaction.

When the LOI (results presented in Figure S5 in the Supplementary Material) and carbonate content (results from calcimeter test) of carbonated wollastonite are compared (Figure S6 in the Supplementary Material), they show a nearly identical trend. As the main purpose of conducting both tests was to validate the reliability of such analysis methods, the consistency in these two results shows that the CO_2 content and carbonate content have a proportional relationship, as expected. According to Figure S5c, slurry carbonated wollastonite had CO_2 content ranging between 0.77–1.02 wt%. Some of these values are lower than the CO_2 content of unreacted wollastonite, which is 0.80 wt%. As the same results were seen in the calcimeter test, it can be concluded that carbonation did not occur and rather the decomposition of carbonates via weathering happened during slurry carbonation. The reduced pH in slurry carbonation of wollastonite is thus only attributable to the mineral losing basicity (and its surface becoming more silica rich) rather than the formation of carbonates.

According to Figure 7a, wollastonite sequestered a net amount of 231 $g_{carbonate}/kg_{sample}$ when it was carbonated using the pressurized carbonation method with ultrapure water as solvent. With the use of 0.64 M NaOH instead of ultrapure water, the carbonate content slightly increases by a further 25 g/kg. Compared to wollastonite, both kimberlite and heat-treated kimberlite carbonated to a significantly more limited extent, though heat-treatment was confirmed to enhance carbonation performance. Kimberlite sequestered net carbonate content of 1 and 27 g/kg through pressurized carbonation using ultrapure water and 0.64 M NaOH, respectively, while heat-treated kimberlite sequestered 17 and 46 g/kg, respectively. Kimberlite, which has a more complex composition of different minerals compared to wollastonite, was predicted to carbonate less effectively. Moreover, wollastonite is known to be relatively more reactive than other natural silicates (i.e., olivine ($(Mg,Fe)_2SiO_4$) and serpentine ($Mg_3Si_2O_5(OH)_4$)) due to the Ca atom that is less tightly bound to valence electron than the Mg atom. It is important to note that the use of NaOH instead of ultrapure water helped in achieving an improved carbonation extent. The net increase in carbonate content was 11% in wollastonite carbonation, and the value nearly doubled in kimberlite carbonation by using 0.64 M NaOH. The role of NaOH is providing the buffer effect to acidic CO_2 saturated water (pH < 4). NaOH improved kimberlite carbonation more effectively than that of wollastonite since the latter has greater initial basicity (10.0 versus 9.0–9.2), so acts as a more effective solid buffer.

Figure 7b shows the $LOI_{300–950°C}$ of the pressurized slurry carbonated samples from the furnace test. The trend in the numerical values agrees with the results of the calcimeter test, where wollastonite significantly carbonated better than the kimberlite during both forms of pressurized carbonation, and the use of 0.64 M NaOH and heat-treatment of kimberlite proved critical to improving carbonation of kimberlite tailings in pressurized carbonation.

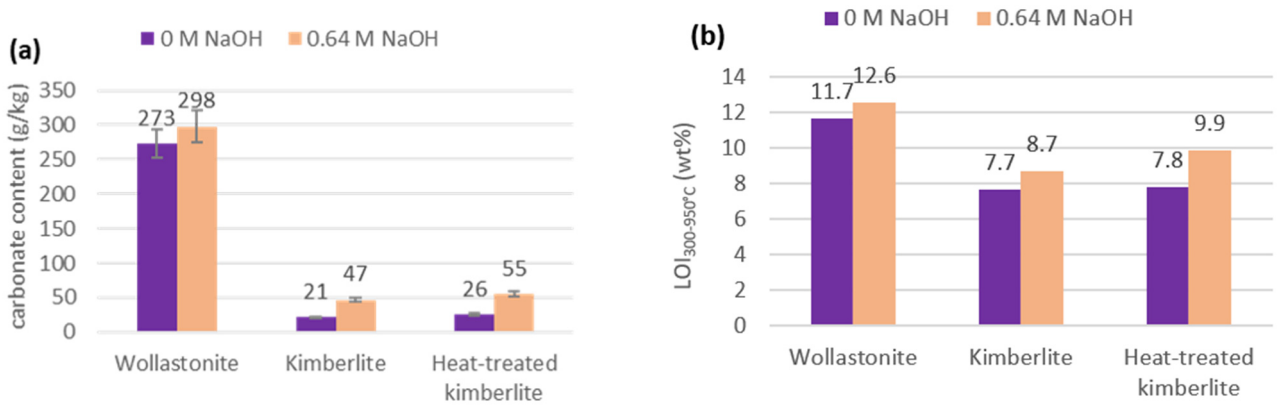

Figure 7. (**a**) Carbonate content (calcimeter mean accuracy: ±7.6%) and (**b**) $LOI_{300–950°C}$ of carbonated wollastonite and kimberlite through pressurized (4 h, 200 °C, 60 bar CO_2). Carbonate content and CO_2 content ($LOI_{300–950°C}$) of unreacted wollastonite are 41.7 g/kg and 0.80 wt%, respectively. Carbonate content and CO_2 content ($LOI_{300–950°C}$) of unreacted kimberlite and heat-treated kimberlite are 19.5 g/kg and 7.3 wt%, and 9.0 g/kg and 4.7 wt%, respectively.

3.3. XRD Analysis

XRD was used to identify mineral phases that formed through weathering and carbonation. Figures 8–10 show the XRD diffractograms of the unreacted materials and the peaks that indicate the crystalline carbonate phases that appeared after carbonation. In the XRD analysis of incubator carbonated kimberlite (Figure 8), formation of hydrated magnesium carbonates, nesquehonite ($MgCO_3 \cdot 3H_2O$), and lansfordite ($MgCO_3 \cdot 5H_2O$), was shown in most samples. Formation of nesquehonite and lansfordite occurring during the incubator carbonation, which was conducted at 35 and 50 °C, was expected as they have been reported to precipitate at temperatures ranging from 25 and 55 °C in published studies [29,30]. Their formation is predicted to have resulted by the transformation of Mg-containing mineral phases, such as serpentine ($Mg_3(Si_2O_5)(OH)_4$) and forsterite (Mg_2SiO_4) that exist in the unreacted kimberlite (Figure 8). Specifically, carbonation of serpentine was predicted [31], which would result in formation of magnesite after carbonation [32]. The carbonation of serpentine is predicted to have been limited by the availability of Mg which is controlled by structural disorder [20]. This is one of the reasons for testing the effect of heat treatment on kimberlite carbonation. Precipitation of hydromagnesite ($Mg_5(CO_3)_4(OH)_2 \cdot 4H_2O$) and magnesite ($MgCO_3$) was not detected as they are more stable polymorphs of magnesium carbonates, that form at higher temperatures of 60–95 °C and 105 °C, respectively [30]. Furthermore, precipitation of calcite ($CaCO_3$) may have occurred during incubator carbonation of kimberlite, but to low levels (the main calcite peak at 29.40° is barely perceptible). It is also possible that some amorphous carbonates may have formed, which are undetectable by XRD, as mild conditions have been used.

Figure 9b,c shows examples of XRD diffractograms of incubator carbonated wollastonite, to be compared to the diffractogram of unreacted wollastonite (Figure 9a). In all incubator carbonated wollastonite samples, the formation of calcite was observed, and in some, the formation of aragonite was also observed. These carbonates have resulted from the weathering of the wollastonite (Ca-source) and diopside (Mg-source that favors aragonite formation [25]) phases. Figure 9c, where aragonite was observed, corresponds to the sample carbonated at elevated temperature (50 °C), and it is known that aragonite is the high-temperature polymorph of calcium carbonate [25]. In all cases, vaterite peaks were not detected. This informs that the incubator carbonation method with the reaction conditions used in this research leads to the complete transformation of metastable vaterite into calcite. The absence of vaterite formation agrees with the results obtained in a published study that elucidated that this complete transformation is achieved at 25 °C [33]. Aragonite remains in the carbonated wollastonite as aragonite completely transforms into calcite at much higher temperatures (above 300 °C) [33]. Due to the diopside composition in the unreacted

wollastonite ore, it was possible that the formation of magnesium carbonates could have occurred during carbonation. However, this is not confirmed according to the results of XRD (Figure 9) and can be explained by diopside being less reactive [10] to weathering and carbonation compared to wollastonite mineral, which is predominant in the tested ore. Moreover, it is understood that there is good correlation between the results of the furnace and calcimeter tests and the polymorphs of calcium carbonates formed. In slurry carbonation, as expected from previous test results, carbonates did not form according to the XRD diffractograms generated (Figure 9d corresponds to slurry carbonated wollastonite at 60 °C for 4 h). Likewise, in terms of correlation, the peaks of calcite and aragonite in Figure 9c are relatively large (e.g., when compared to Figure 9b, and other diffractograms obtained and not shown), which is in agreement with Figures 6c and S5.

Figure 9e,f shows the XRD diffractogram of pressurized carbonated wollastonite. As can be seen, both calcite and aragonite formed as a result of carbonate precipitation for both experiments (using ultrapure water and 0.64 M NaOH). It is observed that the main calcite peak at 29.40° is noticeably taller in Figure 9f than in Figure 9e, though conversely the aragonite main peak at 26.22° is slightly higher in Figure 9e than in Figure 9f. These slight differences are in line with the calcimetry and furnace test results of Figure 7. It should be noted that in the XRD diffractograms of the carbonated wollastonite, the peaks of the wollastonite phase (main peak at 23.20°) that exist in the diffractogram of unreacted wollastonite are much smaller or have nearly disappeared, while the peaks of the diopside phase (main peak at 29.85°, but more visible secondary peak at 35.48°) still exist more evidently. This confirms that the wollastonite phase is much more reactive to carbonation compared to the diopside.

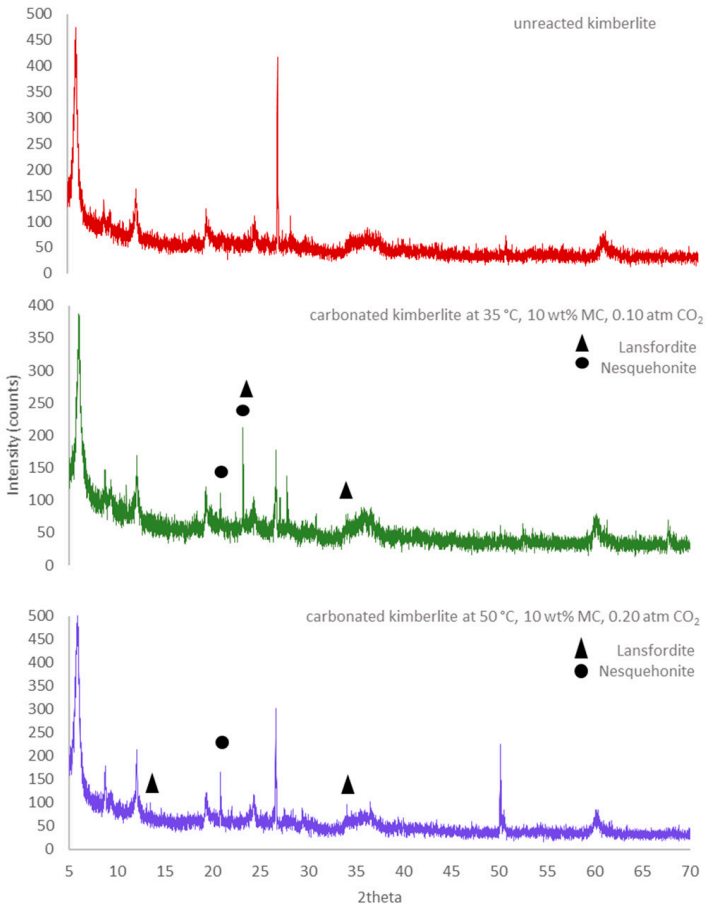

Figure 8. XRD diffractograms of unreacted kimberlite (**top**) and incubator carbonated (144 h) kimberlite at 35 °C, 10 wt% moisture content and 0.10 atm CO_2 (**middle**), and at 50 °C, 10 wt% moisture content, and 0.20 atm CO_2 (**bottom**).

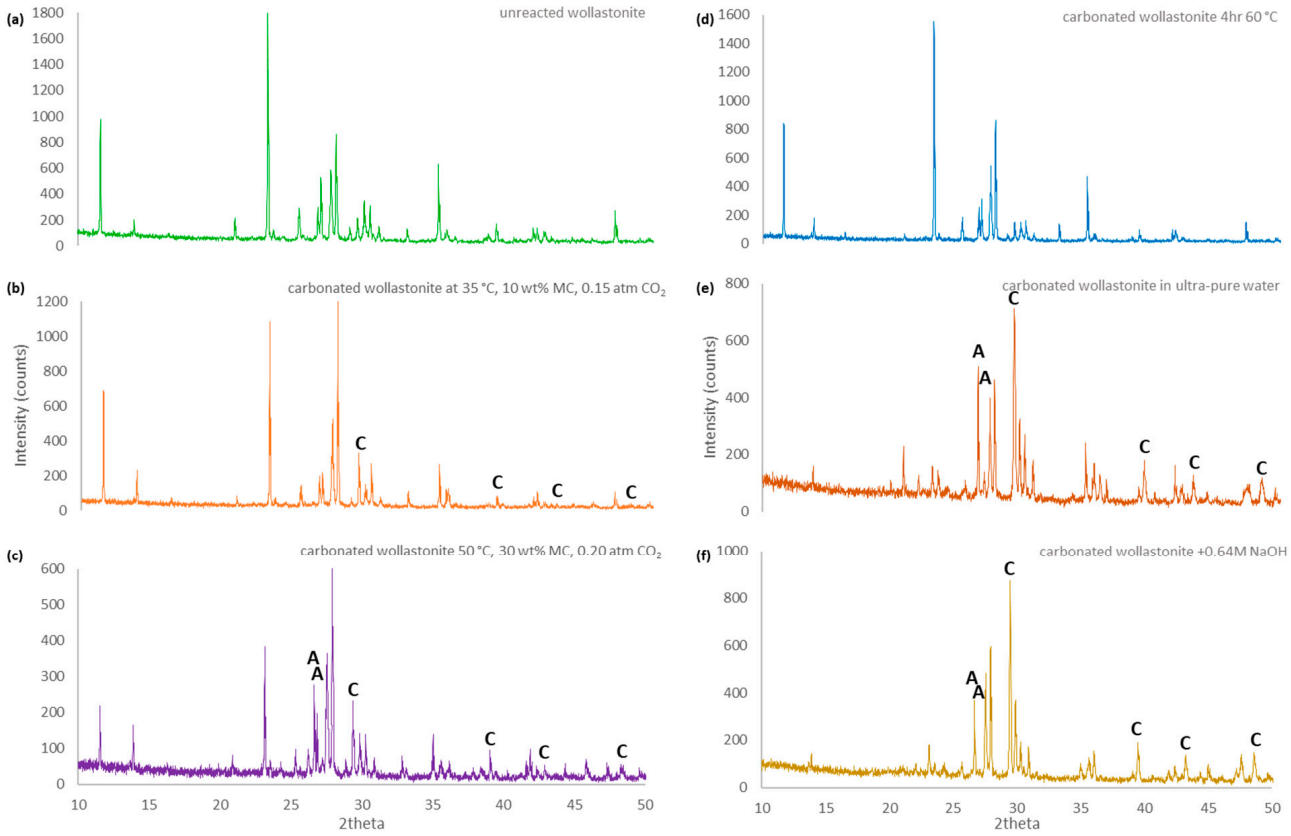

Figure 9. XRD diffractograms of: (**a**) unreacted wollastonite; incubator carbonated (144 h) wollastonite at 35 °C, 10 wt% moisture content, and 0.15 atm CO_2 (**b**) and at 50 °C, 30 wt% moisture content, and 0.20 atm CO_2 (**c**); (**d**) slurry carbonated wollastonite; pressurized slurry carbonated wollastonite at 200 °C and 60 bar in ultrapure water (**e**) and in 0.64 M NaOH (**f**). The letters **A** and **C** indicate peak locations of aragonite ($CaCO_3$) and calcite ($CaCO_3$), respectively.

Figure 10a,b reveal the XRD diffractograms of kimberlite carbonated in a pressurized slurry using ultrapure water and adding 0.64 M of NaOH. As shown in the patterns, the carbonated kimberlite in ultra-pure exhibited lansfordite and nesquehonite. It is important to mention that above 50 °C, nesquehonite tends to transform into hydromagnesite due to its influenced stability by the loss of water from the system. However, no hydromagnesite peaks were detected in Figure 10a, but this carbonate was observed in Figure 10b. The larger carbonate peaks in Figure 10a versus Figure 10b are following the greater carbonate content and LOI presented in Figure 7 when using NaOH.

Figure 10c,d discloses XRD diffractograms of heat-treated kimberlite carbonated in pressurized slurry in ultrapure water and 0.64 M NaOH. The sample reacting in ultra-pure only presented the three aforementioned carbonates: lansfordite, nesquehonite, and hydromagnesite. After adding NaOH, heat-treated carbonated kimberlite still presents nesquehonite and hydromagnesite, the former with taller peaks than the other three subfigures of Figure 10 (lansfordite is also possibly present, though only a single peak is visible). Once again, these results are in line with the heat-treated kimberlite carbonated in NaOH having achieve the highest carbonate content and LOI (Figure 7). Notable, this sample also exhibited an important peak that neared 2000 counts, which correspond to a zeolite phase. The formation of zeolite can be explained by the presence of silica and aluminum from the kimberlite and sodium from the NaOH and the greater reactivity of kimberlite samples after the heat treatment, which under hydrothermal conditions can lead to the formation of crystalline zeolite phases [34].

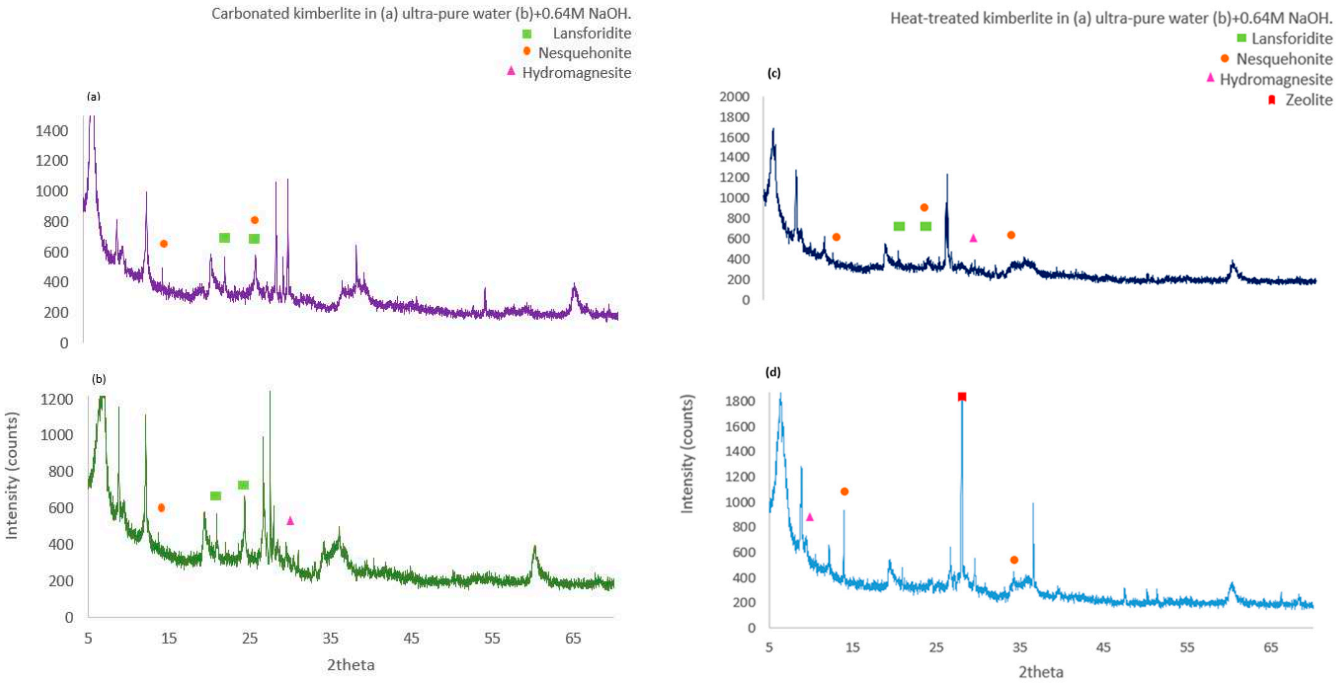

Figure 10. XRD diffractograms of: kimberlite carbonated at 200 °C and 60 bar in ultrapure water (**a**) and in 0.64 M NaOH (**b**); heat-treated kimberlite carbonated at 200 °C and 60 bar in ultrapure water (**c**) and in 0.64 M NaOH (**d**).

3.4. Perspectives on Tailings and Ore Carbonation

The attractive aspect of mine tailings for mineral carbonation is that these rocks are already finely crushed and milled for other value recovery reasons, so they are ready to be carbonated. Still, tailings need to have both a reasonably high capacity for a CO_2 update (based on chemical composition) and reasonable high reactivity towards weathering and carbonation (based on mineral composition and mineral assemblage in particles). In this study, kimberlite meets the former condition, but its potential for accelerated carbonation is hampered by the latter. Even considering the highest carbonation extent herein achieved, resulting in 55 g of $CaCO_3$-equivalent carbonate formation per kilogram, this still is below 10% of conversion compared to the maximal capacity of this tailing (577 g of $CaCO_3$-equivalent per kilogram, assuming the chemical formula of kimberlite as $Mg_{0.846}Al_{0.165}Fe_{0.147}Ca_{0.067}SiO_{3.381}$). A comparison of LOI can be made with the work of Ryu et al. [32], who experimented with heat-treated (650 °C for 2 h) serpentine carbonation under intensified conditions (30 bar CO_2, 290 °C, 100 rpm, 5 h). The highest LOI between 300 °C and 950 °C in that study was approximately 16%, compared to 9.9% in the present study, in both cases with the use of NaOH. The results are comparable when considering the higher temperature and longer time used in the cited study. In addition, it is possible that the mineral assemblages of kimberlite hinder its reactivity, and this micro-structural aspect should be subject to further research.

Turning to wollastonite ore carbonation, the present results are encouraging in terms of the high CO_2 uptake of this material under both incubator and pressurized slurry carbonation, even without the use of NaOH, which simplifies and economizes the process. Evidently, ores must be mined, crushed, and milled for use in ex-situ accelerated carbonation, so the net CO_2 sequestration will be lower than the values directly measured, and life-cycle analysis and costing should be performed to resolve the process conditions that are both technically feasible and CO_2-negative. In a similar analysis done for kimberlite, the maximal capacity of this ore is 535 g $CaCO_3$-equivalent per kilogram (assuming the chemical formula of wollastonite as $Ca_{0.609}Mg_{0.132}Al_{0.091}Fe_{0.024}SiO_{2.914}$). Hence, the wollastonite ore conversion peaked at 44.3% in the incubator tests (237 g $CaCO_3$-equivalent per kilogram), and 55.7% in the pressurized slurry carbonation tests (298 g $CaCO_3$-equivalent per

kilogram). Ding et al. [13] summarized the conversions achieved in various studies on wollastonite carbonation, which ranged from 4 to 91.1%. However, some of those experiments were conducted in two steps (leaching in acid followed by buffered carbonation), and some were conducted at very high pressure (150 to 250 bar). The two closest reaction conditions to the current study achieved 45% and 80% conversion. These results are in line with the present results, but it is important to note that those studies used refined wollastonite (i.e., processed wollastonite that is refined to yield high-grade products). Considering that the present study used an ore with a relatively high content of other less reactive minerals (such as diopside, as inferred from XRD analysis), the conversions obtained in the present study suggest that mineral assemblage is not an issue for wollastonite ore. This has been observed in our previous studies via SEM (scanning electron microscopy) analysis [21], wherein it was observed that individual wollastonite ore particles are largely composed of single minerals, thus secondary minerals do not hinder the reactivity of the more reactive ones, particularly the wollastonite phase.

4. Conclusions

With the continuous concerns regarding climate change due to greenhouse gas emissions, the release of CO_2 must be controlled by a method that safely and permanently sequesters CO_2. Mineral carbonation is a promising solution because of the abundant alkaline mineral available on the earth's crust. Canada's extensive alkaline mineral reserves have the potential to be utilized in the sequestration of a large fraction of emission through engineered accelerated mineral carbonation. The purpose of this research was to evaluate the potential of kimberlite mine tailing from the Northwest Territories (Canada), and wollastonite ore sourced from Ontario (Canada) to sequester CO_2 under mild to intensified conditions. The various accelerated weathering and carbonation methods were conducted, and the carbonation performance and mineralogy were evaluated by pH test, furnace test, calcimeter test, and XRD analysis. The overall conclusion from this work is that wollastonite (rich in fast-weathering calcium silicate) is more suitable for accelerated carbonation than kimberlite (containing slow-weathering hydrated magnesium silicates and aluminosilicates) when only its capability to capture CO_2 is considered. However, the potential of utilizing carbonated kimberlite as a building material was verified in our prior work [35], which opens opportunities to avoid the environmental impact of tailings ponds, while covering the processing cost of sequestering CO_2. Hence, the full life cycle of the sourced mineral should be considered when evaluating the effectiveness and benefits of mineral carbonation processes. Kimberlite also has the potential to be utilized for enhanced weathering as a negative emissions technology in industrial, agricultural or urban settings [31,36], where low processing costs compensate for slow reaction.

The pH test results of the carbonated kimberlite and wollastonite were not sufficient to confidently elucidate the effect of carbonation on their basicity. This was mainly because the kimberlite and wollastonite have pH levels similar to typical carbonates, and also because some tests resulted in weathering reactions rather than carbonation reactions. The furnace test indicated that kimberlite sequestered a minimal amount of CO_2 (<1 wt%), while naturally more reactive wollastonite showed a significant amount of carbonates formation through incubator carbonation. In slurry carbonation of kimberlite, the samples that received heat treatment sequestered an average of 1 wt% CO_2, while most samples that were not heat-treated did not show an indication of CO_2 sequestration. Heat treatment was used to dehydroxylate the serpentine mineral in kimberlite as an attempt to increase its reactivity. Moreover, the slurry carbonation of wollastonite performed very poorly. The limiting factors of slurry carbonation experiments include short duration (1 to 4 h), high liquid to solid ratio (20:1), and low pH value of the aqueous phase given the higher CO_2 partial pressure (1 atm) of these experiments versus that of incubator carbonation (0.10 to 0.20 atm CO_2, 10 to 30 wt% moisture, for 144 h). It is likely that under slurry carbonation the solution does not become as concentrated with weathered alkaline earth metals as in

incubator carbonation, given the much higher liquid-to-solid ratio of the former, and this can contribute to hindering the precipitation of solid carbonates.

In the pressurized slurry carbonation, wollastonite again showed better carbonation performance than kimberlite. When the amounts of carbonates formed by wollastonite samples through incubator and pressurized slurry carbonation are compared, even at optimum conditions of incubator carbonation, greater amounts of carbonates were formed by pressurized slurry carbonation. Far more elevated temperature and CO_2 pressure are driving forces to a greater extent of weathering, and in turn precipitation of solid carbonates from the solution saturated with alkaline earth elements. However, for industrial implementation of the methods, the energy usage and cost-effectiveness to maintain the intensified reaction conditions and equipment used for pressurized carbonation should be considered.

The XRD analyses identified the products of the carbonation processes. For carbonated kimberlite, the formation of lansfordite was seen in all carbonation methodologies, while nesquehonite was more commonly observed under milder carbonation conditions, and hydromagnesite was only seen under intensified conditions. According to Hopkinson et al. [37], nesquehonite is metastable and converts to hydromagnesite at an accelerated rate at elevated temperatures, which can explain the observations in the present study. In terms of calcium carbonates, calcite formed during incubator and pressurized carbonation of wollastonite, with aragonite also observed at higher temperatures, while carbonate formation was absent during slurry carbonation, which as previously discussed in an indication that the slurry reaction was more akin to weathering than to carbonation.

This research is still ongoing and will continue to evaluate kimberlite and wollastonite carbonation utilizing other experimental methods. We are evaluating how ball milling during mineral carbonation affects the carbonation rate, extent, and reactivity of mineral phases. We are also evaluating the energy demand and life-cycle net carbon footprint of mineral carbonation processes considering the availability of diverse types of minerals and the end-use of the carbonated minerals in building materials where they can create emissions off-sets by partly replacing cement and fine aggregates.

Supplementary Materials: The following are available online at https://www.mdpi.com/article/10.3390/cryst11121584/s1, Figure S1: pH of carbonated kimberlite after incubator carbonation (24 h and 144 h) at 10 % CO_2 and reaction temperatures of (a) 35 °C and (b) 50 °C, and at 20 % CO_2 and reaction temperatures of (c) 35 °C and (d) 50 °C; where MC represents moisture content. pH of unreacted kimberlite is 9.2. The value of 7.64 in Figure S1c is considered an outlier. Figure S2: pH of carbonated wollastonite after incubator carbonation (24 h and 144 h) at 15 % CO2 and reaction temperatures of (a) 35 °C and (b) 50 °C and at 20 % CO_2 and reaction temperatures of (c) 35 °C and (d) 50 °C; where MC represents moisture content. pH of unreacted wollastonite is 10.0. Figure S3: pH of carbonated (a) kimberlite, (b) heat treated kimberlite, and (c) wollastonite after slurry carbonation in ultrapure water. pH of unreacted kimberlite, heat treated kimberlite, and wollastonite are 9.2, 9.0, and 10.0, respectively. Figure S4: pH of (a) kimberlite, (b) heat treated kimberlite, and (c) wollastonite after slurry carbonation in 0.64 M NaOH. pH of unreacted kimberlite, heat treated kimberlite, and wollastonite are 9.2, 9.0, and 10.0, respectively. Figure S5: CO2 content ($LOI_{300–950°C}$) of incubator carbonated (144 hr) wollastonite at (a) 35 °C and (b) 50 °C and slurry carbonated wollastonite in (c) ultrapure water and (d) NaOH. CO_2 content ($LOI_{300–950°C}$) of unreacted wollastonite is 0.80 wt%. Figure S6: Comparison between calcimeter and furnace test results. Wollastonite carbonated using incubator carbonation at (a) 35 °C and (b) 50 °C.

Author Contributions: Conceptualization, R.M.S.; methodology, Y.E.C., S.C. and H.F., and R.M.S.; investigation, Y.E.C., and H.F.; writing—original draft preparation, Y.E.C.; writing—review and editing, S.C. and R.M.S.; supervision, R.M.S.; project administration, R.M.S.; funding acquisition, S.C. and R.M.S. All authors have read and agreed to the published version of the manuscript.

Funding: This research was funded by the Mitacs Globalink program and the Natural Sciences and Engineering Research Council of Canada (NSERC) Discovery Grant.

Institutional Review Board Statement: Not applicable.

Informed Consent Statement: Not applicable.

Data Availability Statement: Data available upon request.

Conflicts of Interest: The authors declare no conflict of interest.

References

1. UNFCCC Secretariat Welcomes IPCC's Global Warming of 1.5 °C Report. Available online: https://unfccc.int/news/unfccc-secretariat-welcomes-ipcc-s-global-warming-of-15degc-report (accessed on 11 December 2021).
2. Pan, S.Y.; Chen, Y.H.; Fan, L.-S.; Kim, H.; Gao, X.; Ling, T.-C.; Chiang, P.-C.; Pei, S.-L.; Gu, G. CO_2 mineralization and utilization by alkaline solid wastes for potential carbon reduction. *Nat. Sustain.* **2020**, *3*, 399–405. [CrossRef]
3. Snæbjörnsdóttir, S.Ó.; Sigfússon, B.; Marieni, C.; Goldberg, D.; Gislason, S.R.; Oelkers, E.H. Carbon dioxide storage through mineral carbonation. *Nat. Rev. Earth Environ.* **2020**, *1*, 90–102. [CrossRef]
4. Zhang, N.; Santos, R.M.; Smith, S.M.; Šiller, L. Acceleration of CO_2 mineralisation of alkaline brines with nickel nanoparticles catalysts in continuous tubular reactor. *Chem. Eng. J.* **2019**, *377*, 120479. [CrossRef]
5. Boyjoo, Y.; Pareek, V.; Liu, J. Synthesis of micro and nano-sized calcium carbonate particles and their applications. *J. Mater. Chem. A* **2014**, *2*, 14270–14288. [CrossRef]
6. Ncongwane, M.; Broadhurst, J.; Petersen, J. Assessment of the potential carbon footprint of engineered processes for the mineral carbonation of PGM tailings. *Int. J. Greenh. Gas Control* **2018**, *77*, 70–81. [CrossRef]
7. Huijgen, W.; Comans, R. *Carbon Dioxide Sequestration by Mineral Carbonation*; Energy Research Centre of the Netherlands (ECN): Petten, The Netherlands, 2003.
8. Fricker, K.J.; Park, A.H. Effect of H_2O on $Mg(OH)_2$ carbonation pathways for combined CO_2 capture and storage. *Chem. Eng. Sci.* **2013**, *100*, 332–341. [CrossRef]
9. Nduagu, E.; Bergerson, J.; Zevenhoven, R. Life cycle assessment of CO_2 sequestration in magnesium silicate rock—A comparative study. *Energy Convers. Manag.* **2012**, *55*, 116–126. [CrossRef]
10. Monasterio-Guillot, L.; Fernandez-Martinez, A.; Ruiz-Agudo, E.; Rodriguez-Navarro, C. Carbonation of calcium-magnesium pyroxenes: Physical-chemical controls and effects of reaction-driven fracturing. *Geochim. Cosmochim. Acta* **2021**, *304*, 258–280. [CrossRef]
11. Wang, F.; Dreisinger, D.; Jarvis, M.; Hitchins, T. Kinetic evaluation of mineral carbonation of natural silicate samples. *Chem. Eng. J.* **2021**, *404*, 126522. [CrossRef]
12. Ashraf, W.; Olek, J. Elucidating the accelerated carbonation products of calcium silicates using multi-technique approach. *J. CO2 Util.* **2018**, *23*, 61–74. [CrossRef]
13. Ding, W.; Fu, L.; Ouyang, J.; Yang, H. CO_2 mineral sequestration by wollastonite carbonation. *Phys. Chem. Miner.* **2014**, *41*, 489–496. [CrossRef]
14. Ding, W.; Yang, H.; Ouyang, J.; Long, H. Modified wollastonite sequestrating CO_2 and exploratory application of the carbonation products. *RSC Adv.* **2016**, *6*, 78090–78099. [CrossRef]
15. Yadav, S.; Mehra, A. Mathematical modelling and experimental study of carbonation of wollastonite in the aqueous media. *J. CO2 Util.* **2019**, *31*, 181–191. [CrossRef]
16. Di Lorenzo, F.; Ruiz-Agudo, C.; Ibañez-Velasco, A.; Gil-San Millán, R.; Navarro, J.; Ruiz-Agudo, E.; Rodriguez-Navarro, C. The Carbonation of Wollastonite: A Model Reaction to Test Natural and Biomimetic Catalysts for Enhanced CO_2 Sequestration. *Minerals* **2018**, *8*, 209. [CrossRef]
17. Min, Y.; Li, Q.; Voltolini, M.; Kneafsey, T.; Jun, Y.-S. Wollastonite Carbonation in Water-Bearing Supercritical CO_2: Effects of Particle Size. *Environ. Sci. Technol.* **2017**, *51*, 13044–13053. [CrossRef]
18. Hamilton, J.L.; Wilson, S.A.; Morgan, B.; Harrison, A.; Turvey, C.C.; Paterson, D.; Dipple, G.M.; Southam, G. Accelerating Mineral Carbonation in Ultramafic Mine Tailings via Direct CO_2 Reaction and Heap Leaching with Potential for Base Metal Enrichment and Recovery. *Econ. Geol.* **2020**, *115*, 303–323. [CrossRef]
19. Ramli, N.A.A.; Kusin, F.M.; Molahid, V.L.M. Influencing Factors of the Mineral Carbonation Process of Iron Ore Mining Waste in Sequestering Atmospheric Carbon Dioxide. *Sustainability* **2021**, *13*, 1866. [CrossRef]
20. Dlugogorski, B.Z.; Balucan, R.D. Dehydroxylation of serpentine minerals: Implications for mineral carbonation. *Renew. Sustain. Energy Rev.* **2013**, *32*, 353–367. [CrossRef]
21. Haque, F.; Santos, R.M.; Chiang, Y.W. Optimizing inorganic carbon sequestration and crop yield with wollastonite soil amendment in a microplot study. *Front. Plant Sci.* **2020**, *11*, 1012. [CrossRef]
22. Bodor, M.; Santos, R.; Kriskova, L.; Elsen, J.; Vlad, M.; Van Gerven, T. Susceptibility of mineral phases of steel slags towards carbonation: Mineralogical, morphological and chemical assessment. *Eur. J. Mineral.* **2013**, *25*, 533–549. [CrossRef]
23. Santos, R.M.; Van Bouwel, J.; Vandevelde, E.; Mertens, G.; Elsen, J.; Van Gerven, T. Accelerated mineral carbonation of stainless steel slags for CO_2 storage and waste valorization: Effect of process parameters on geochemical properties. *Int. J. Greenh. Gas Control* **2013**, *17*, 32–45. [CrossRef]
24. Santos, R.M.; Bodor, M.; Dragomir, P.N.; Vraciu, A.G.; Vlad, M.; Van Gerven, T. Magnesium chloride as a leaching and aragonite-promoting self-regenerative additive for the mineral carbonation of calcium-rich materials. *Miner. Eng.* **2014**, *59*, 71–81. [CrossRef]

25. Santos, R.M.; van Audenaerde, A.; Chiang, Y.W.; Iacobescu, R.I.; Knops, P.; van Gerven, T. Nickel extraction from olivine: Effect of carbonation pre-treatment. *Metals* **2015**, *5*, 1620–1644. [CrossRef]
26. Dudhaiya, A.; Haque, F.; Fantucci, H.; Santos, R.M. Characterization of physically fractionated wollastonite-amended agricultural soils. *Minerals* **2019**, *9*, 635. [CrossRef]
27. Soong, Y.; Goodman, A.L.; Mccarthy-Jones, J.R.; Baltrus, J.P. Experimental and simulation studies on mineral trapping of CO_2 with brine. *Energy Convers. Manag.* **2004**, *45*, 1845–1859. [CrossRef]
28. Li, Y.; Chen, X.; Huang, W.; Yang, J. Below the Room Temperature Measurements of CO_2 Solubilities in Six Physical Absorbents. *J. Chem. Thermodyn.* **2018**, *122*, 113–141. [CrossRef]
29. Morgan, B.; Wilson, S.A.; Madsen, I.C.; Gozukara, Y.M.; Habsuda, J. Increased thermal stability of nesquehonite ($MgCO_3 \cdot 3H_2O$) in the presence of humidity and CO_2: Implications for low-temperature CO_2 storage. *Int. J. Greenh. Gas Control* **2015**, *39*, 366–376. [CrossRef]
30. Zhang, Z.; Zheng, Y.; Ni, Y.; Liu, Z.; Chen, J.; Liang, X. Temperature-and pH-dependent morphology and FT-IR analysis of magnesium carbonate hydrates. *J. Phys. Chem. B* **2006**, *110*, 12969–12973. [CrossRef] [PubMed]
31. Mervine, E.M.; Wilson, S.A.; Power, I.M.; Dipple, G.M.; Turvey, C.C.; Hamilton, J.L.; Vanderzee, S.; Raudsepp, M.; Southam, C.; Matter, J.M.; et al. Potential for offsetting diamond mine carbon emissions through mineral carbonation of process kimberlite: An assessment of De Beers mine sites in South Africa and Canada. *Miner. Petrol.* **2018**, *112*, 755–765. [CrossRef]
32. Ryu, K.W.; Jo, H.; Choi, S.H.; Chae, S.C.; Jang, Y.N. Changes in mineral assemblages during serpentine carbonation. *Appl. Clay Sci.* **2016**, *134*, 62–67. [CrossRef]
33. Chang, R.; Kim, S.; Lee, S.; Choi, S.; Kim, M.; Park, Y. Calcium Carbonate Precipitation for CO_2 Storage and Utilization: A Review of the Carbonate Crystallization and Polymorphism. *Front. Energy Res.* **2017**, *5*, 17. [CrossRef]
34. Georgakopoulos, E.; Santos, R.M.; Chiang, Y.W.; Manovic, V. Two-way valorization of blast furnace slag: Synthesis of precipitated calcium carbonate and zeolitic heavy metal adsorbent. *J. Vis. Exp.* **2017**, *120*, e55062. [CrossRef] [PubMed]
35. Chakravarthy, A.C.; Chalouati, S.; Chai, Y.E.; Fantucci, H.; Santos, R.M. Valorization of Kimberlite Tailings by Carbon Capture and Utilization (CCU) Method. *Minerals* **2020**, *10*, 611. [CrossRef]
36. Haque, F.; Santos, R.M.; Chiang, Y.W. Urban farming with enhanced rock weathering as a prospective climate stabilization wedge. *Environ. Sci. Technol.* **2021**, *55*, 13575–13578. [CrossRef] [PubMed]
37. Hopkinson, L.; Rutt, K.; Cressey, G. The Transformation of Nesquehonite to Hydromagnesite in the System CaO-MgO-H_2O-CO_2: An Experimental Spectroscopic Study. *J. Geol.* **2018**, *116*, 387–400. [CrossRef]